Journal of Power Sources 189 (2009) 706–710

Contents lists available at ScienceDirect

Journal of Power Sources

journal homepage: www.elsevier.com/locate/jpowsour

Short communication

Electrochemical properties of rechargeable aqueous lithium ion batteries with an olivine-type cathode and a Nasicon-type anode

Xiao-Hong Liu, Taishi Saito, Takayuki Doi, Shigeto Okada*, Jun-ichi Yamaki

Institute of Material Chemistry and Engineering Science, Kyushu University, Kasuga Koen 6-1, Kasuga 816-8580, Japan

ARTICLE INFO

Article history:
Received 26 June 2008
Received in revised form 18 August 2008
Accepted 21 August 2008
Available online 27 August 2008

Keywords:
Aqueous lithium ion battery
Olivine
Nasicon

ABSTRACT

Rechargeable aqueous lithium ion batteries have been developed by using olivine $LiMn_{0.05}Ni_{0.05}Fe_{0.9}PO_4$ as cathode material, Nasicon $LiTi_2(PO_4)_3$ as anode material, and saturated Li_2SO_4 solution as electrolyte. The cycling performance and rate capability of these batteries have been investigated. At a current density of 0.2 mA/cm^2, the initial discharge capacity of the battery was approximately 103.9 mAh/g, and the potential plateau was located at 0.92 V. The rate capability of aqueous electrolyte was found to be preferable to that of organic electrolyte. Such inexpensive, secure and high rate rechargeable lithium ion battery should have a potential for use in many applications.

1. Introduction

The coming global energy crisis is compelling people to find energy alternatives. Likewise, how to improve energy efficiency and to make energy infrastructure more secure and reliable are also important areas of concern. Hybrid electric vehicles (HEVs) are significant in addressing the above problems, and much effort has been put into research regarding advanced batteries for HEVs [1–9]. Lithium ion batteries, which are good candidates for such batteries, are an outstanding electrical source and have been commercialized for about 20 years; however, many problems with these batteries still remain. Usually, lithium ion batteries contain flammable organic electrolytes, which tend to easily cause intense smoke or even fire in the case of improper use. Moreover, the cost is too high for making lithium batteries with organic electrolyte in a perfectly dry environment. Therefore, the application of aqueous electrolyte has recently been seen as an attractive alternative, and much attention has been paid to its development [10–15]. Because of the decomposition of water, the most important thing to consider in this development is the selection of cathode and anode active materials. Aqueous cells with $LiMn_2O_4$ and VO_2 as electrode materials and 5 M $LiNO_3$ in water as the electrolyte were first reported [10,11], but the evolution of oxygen at the $Li_{1-x}Mn_2O_4$ electrode in basic electrolyte presented a problem with this design. Rechargeable lithium ion batteries with aqueous electrolyte have also been constructed with $LiNi_{0.81}Co_{0.19}O_2$ as the cathode material and LiV_3O_8 as the anode material within 1 M Li_2SO_4 aqueous electrolyte [12], in that the comparatively sharp inclining/declining charge/discharge curves show a rapid rise/fall in the limit voltage, which in turn leads to reduced capacities. Otherwise, the electrochemical behavior of lithium intercalation compounds such as $LiMnPO_4$ and $LiFePO_4$ within aqueous electrolyte have been investigated [16–19]. As a candidate for the cathode material, the low-cost and environmentally benign olivine $LiFePO_4$ is attractive for many reasons, its rare-metal free composition, its larger gravimetric (Ah/g) and volumetric capacities (Ah/cc), its flat charge/discharge voltage profile, and its excellent thermal and chemical stability at both end members, etc. [20]. To improve the conductivity of the material, many strategies have been employed, including carbon coating, metal doping, and novel synthesis methods. The aqueous battery with olivine cathode and Nasicon anode deserves close attention.

In this paper, the performances of the aqueous Li-ion battery with doped olivine cathode, $LiMn_{0.05}Ni_{0.05}Fe_{0.9}PO_4$ (3.43 V vs. Li^+/Li), and Nasicon anode, $LiTi_2(PO_4)_3$ (2.5 V vs. Li^+/Li) are reported.

2. Experimental

2.1. Preparation of cathode electrode

The doped olivine $LiMn_{0.05}Ni_{0.05}Fe_{0.9}PO_4$ used as cathode active material in this work was prepared by sol–gel method according to reference [21]. Stoichiometric amounts of ferrous sulfate, manganese acetate, nickel acetate, lithium nitrate, and ammonium dihydrogen phosphate were used as starting materials; citric acid

* Corresponding author. Tel.: +81 92 583 7841; fax: +81 92 583 7841.
E-mail address: s-okada@cm.kyushu-u.ac.jp (S. Okada).

0378-7753/$ – see front matter © 2008 Elsevier B.V. All rights reserved.
doi:10.1016/j.jpowsour.2008.08.050

was adopted as a chelating agent. The sol was dried in a vacuum dryer followed by heating at 550 °C for 2 h and 850 °C for 1 h in Ar to avoid the oxidation of ferrous ion. The $LiMn_{0.05}Ni_{0.05}Fe_{0.9}PO_4/C$ was then obtained. In this experiment, the molar ratio of chelating agent to the total metal ion was 1:1, and the molar ratio of (Fe + Mn + Ni):Li:P was 1:1:1. The resulting material was single-phase olivine structure doped with two metals, as was determined by the X-ray diffraction (XRD) pattern. The composite electrodes contained $LiMn_{0.05}Ni_{0.05}Fe_{0.9}PO_4$ as cathode active material (70% by weight), acetylene black (AB, 25% by weight), and polytetrafluoroethylene (PTFE) binder (5% by weight). Any carbothermal treatment was not done for the cathode and anode in this paper. Ti mesh was used as a current collector.

2.2. Preparation of anode electrode

Anode material $LiTi_2(PO_4)_3$ was obtained by a solid reaction of stoichiometric amounts of lithium carbonate, titanium dioxide, and ammonium dihydrogen phosphate. The starting materials were finely ground and then heated gradually to 1000 °C for 45 h in air. The anode electrode was composed of the resulting $LiTi_2(PO_4)_3$ (70% by weight) mixed with AB (25% by weight) by ball-milling, and with PTFE binder (5% by weight).

All the electrode pellets were dried in vacuum before they were assembled into 2032 coin cells with organic electrolyte (1 M $LiPF_6$/EC: DMC = 1:1 vol%) in an Ar glove box, or with aqueous electrolyte (saturated Li_2SO_4 aq.) in air. The electrode materials were identified via field emission scanning electronic microscopy (FESEM, Hatachi 2100) and X-ray diffraction (XRD, Rigaku, RINT2100HLR/PC).

3. Results and discussion

Fig. 1 shows the XRD pattern of as-synthesized $LiMn_{0.05}Ni_{0.05}Fe_{0.9}PO_4/C$ and $LiTi_2(PO_4)_3$, respectively. In Fig. 1(a), all peaks can be indexed to the olivine structure, orthorhombic cell, *Pnma* space group (JCPDS 40-1499). The doped material was well-crystallized in the olivine structure of $LiFePO_4$, and there were no detectable impurity phases. In Fig. 1(b), all the observed reflections can be indexed in the rhombohedral crystal system.

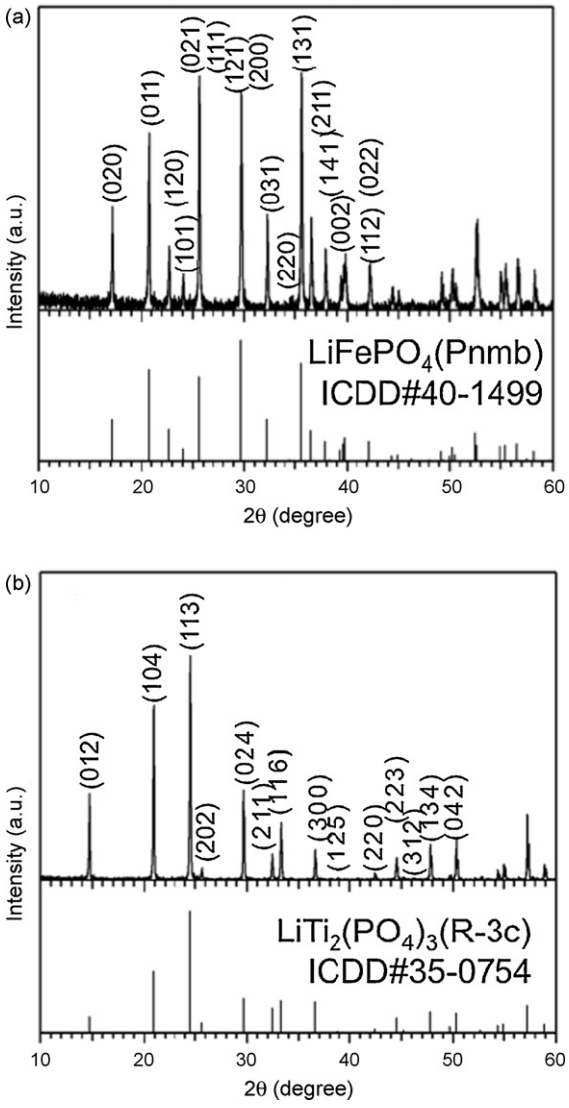

Fig. 1. XRD pattern of (a) $LiMn_{0.05}Ni_{0.05}Fe_{0.9}PO_4$ and (b) $LiTi_2(PO_4)_3$.

Fig. 2 presents FESEM images of the resulting $LiMn_{0.05}Ni_{0.05}Fe_{0.9}PO_4$ and $LiTi_2(PO_4)_3$, respectively. From Fig. 2(a), it can be found that the active particles were surrounded by carbon derived from citric acid, which helps to increase the conductivity of the material, as well as to prevent particle agglomeration when heating at high temperature. The FESEM images of $LiTi_2(PO_4)_3$ are shown in Fig. 2(b). Because the Nasicon material needs to be calcined at high temperature for a long period, the particle size is very large. In addition, by checking the charge/discharge performance, we found that it has large polarization and capacity decline (not shown here). The low intrinsic electronic conductivity of the three-dimensional phosphates always presents this problem. In addition, it has been reported that almost complete reversible insertion of lithium can be obtained by ball-milling $LiTi_2(PO_4)_3$ with carbon during electrode preparation [22]. After ball-milling with carbon, the particle size of $LiTi_2(PO_4)_3$ became smaller, and the active materials were dispersed uniformly in carbon (Fig. 2(c)), which helps to counter the low intrinsic electronic conductivity of this material.

Due to the decomposition of water, the selection of electrode materials is quite important. Fig. 3 shows the stability windows of water at various pH values, as well as charge/discharge voltages for some general cathode and anode active materials. Outside the range of the stability window for water, oxygen or hydrogen evolution will be generated; in addition, the potential range changes with the pH values, according to Nernst equation. Although 4 V cathodes such as $LiMn_2O_4$ or $LiNi_{0.81}Co_{0.19}O_2$ were usually used as cathode in previous papers [10,12,14], the voltage seems to be too high for the aqueous electrolyte. In this paper, we selected olivine $LiFePO_4$ and Nasicon $LiTi_2(PO_4)_3$ as cathode and anode, respectively, because both of them have the two-phase flat charge/discharge voltages within the stability window for water and they are also environmentally benign materials in themselves.

In order to get reference data to compare with aqueous lithium ion batteries, the half cell properties of the each electrode active materials were evaluated in nonaqueous electrolyte, used Li metal as the counter electrode. Fig. 4(a) shows the charge/discharge profile of $LiMn_{0.05}Ni_{0.05}Fe_{0.9}PO_4$, in which the charge and discharge flat plateaus are located at 3.47 V (vs. Li/Li^+) and 3.40 V (vs. Li^+/Li), respectively. There was no capacity decline from the first to the fifth cycle, which indicates that the as-synthesized $LiMn_{0.05}Ni_{0.05}Fe_{0.9}PO_4$ has basically good cycling performance. In addition, according to the voltage range, we determined that the charge/discharge voltage range in neutral aqueous electrolyte should be 0.3–0.6 V (vs. normal hydrogen electrode, NHE), which is safely within the stability window for water. In this range, no

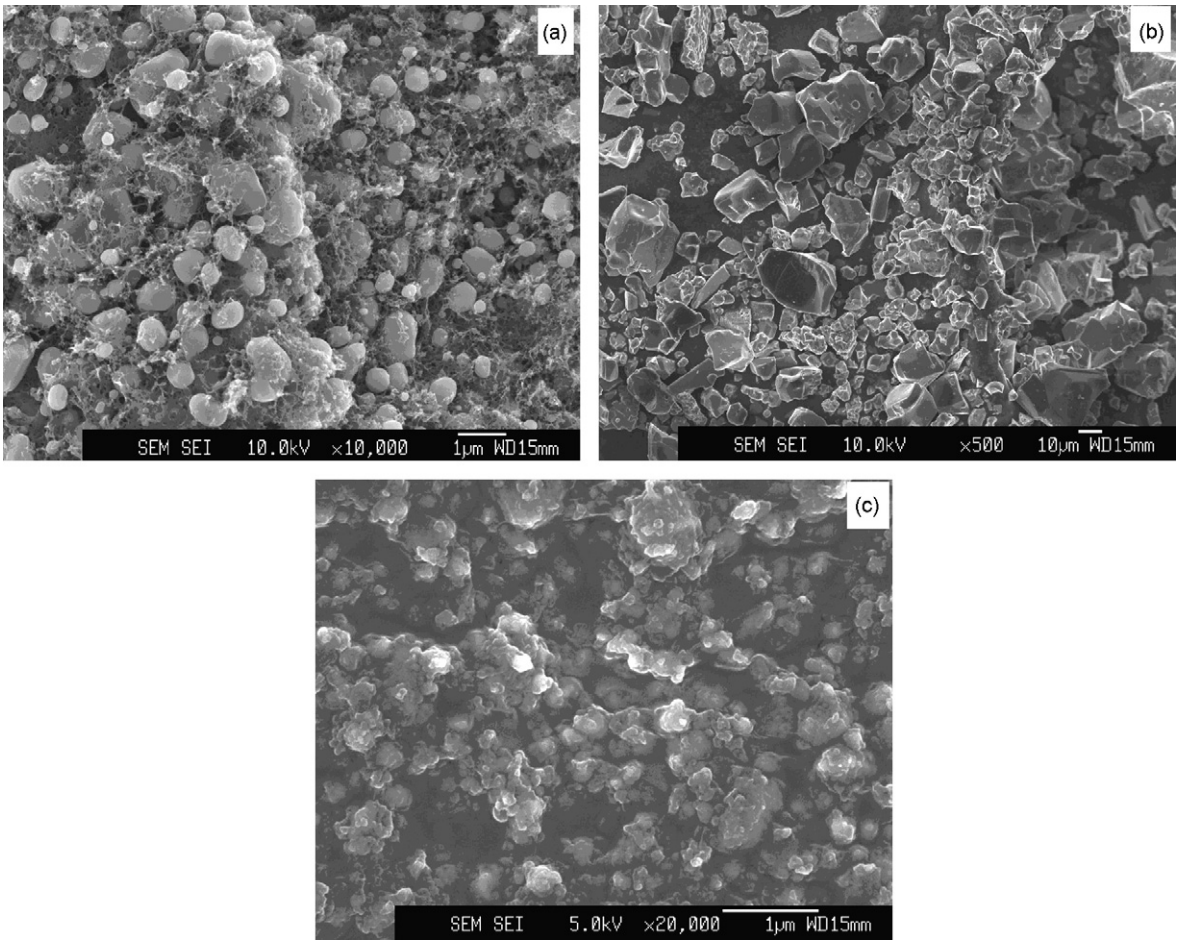

Fig. 2. FESEM images of (a) $LiMn_{0.05}Ni_{0.05}Fe_{0.9}PO_4/C$; (b) $LiTi_2(PO_4)_3$, and (c) $LiTi_2(PO_4)_3$ ball-milled with AB.

oxygen or hydrogen will be generated. The charge/discharge profile of ball-milled $LiTi_2(PO_4)_3$ with Li metal as a counter electrode in organic electrolyte is shown in Fig. 4(b). There was irreversible capacity loss from the first discharge to charge, but from the second cycle, there was almost no capacity decrease, which indicates that the method of ball-milling with carbon is effective in improving the charge/discharge performance of $LiTi_2(PO_4)_3$. In addition, for the discharge/charge equilibrium potentials located at 2.45 V (vs. Li^+/Li), and 2.52 V (vs. Li/Li^+), respectively, the flat voltage plateaus imply a two-phase mechanism for lithium insertion/deinsertion.

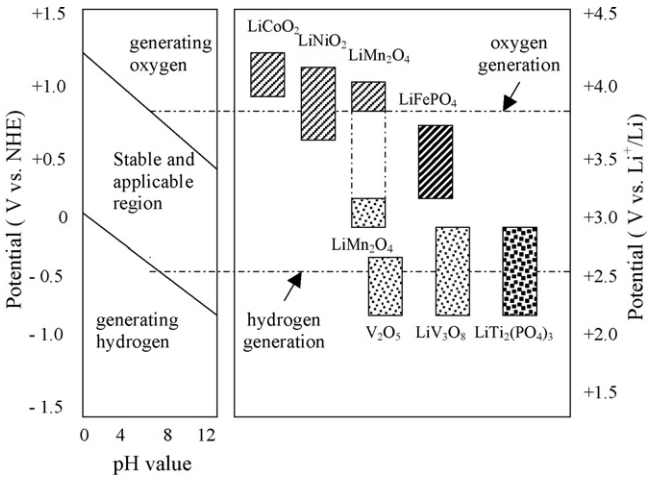

Fig. 3. Potentials for Lithium ion de/intercalation for some selected compounds relative to Li metal (right) and versus NHE (left) for 1 M aqueous solution. The area between the dotted lines represents the stable potential window for water at pH 7.

The charge/discharge performance of $LiMn_{0.05}Ni_{0.05}Fe_{0.9}PO_4//LiTi_2(PO_4)_3$ within aqueous electrolyte has been determined over a potential range between 0.6 V and 1.2 V, and the capacity calculations were based on the weight of cathode active materials. During charging, the lithium ions were extracted from the $LiMn_{0.05}Ni_{0.05}Fe_{0.9}PO_4$ cathode host, making $Li_{1-x}Mn_{0.05}Ni_{0.05}Fe_{0.9}PO_4$, and intercalated into the $LiTi_2(PO_4)_3$ anode, making $Li_{1+x}Ti_2(PO_4)_3$. During discharge, lithium ions were deintercalated from the anode and intercalated into the cathode. According to the potentials of $LiMn_{0.05}Ni_{0.05}Fe_{0.9}PO_4$ and $LiTi_2(PO_4)_3$ (vs. Li^+/Li), respectively, the cell should have a terminal voltage near 1 V. The charge/discharge profile is shown in Fig. 5. In the first cycle, the irreversible capacity was large, maybe due to the irreversible capacity of the anode material $LiTi_2(PO_4)_3$ as shown in Fig. 4(b). If this assumption is not wrong, Li rich $Li_{1+\alpha}Ti_2(PO_4)_3$ should be effective to compensate the irreversible capacity. In the second cycles, the cell showed excellent reversibility, and the capacity declines were very small. The charge/discharge equilibrium potential was located at 0.97 V and 0.92 V, respectively. The flat voltage plateaus and small charge/discharge over potential indicate a two-phase mechanism for lithium insertion/deinsertion in neutral aqueous electrolyte. The clear cutoff voltages provide a charge/discharge voltage range that can avoid the decomposition of water.

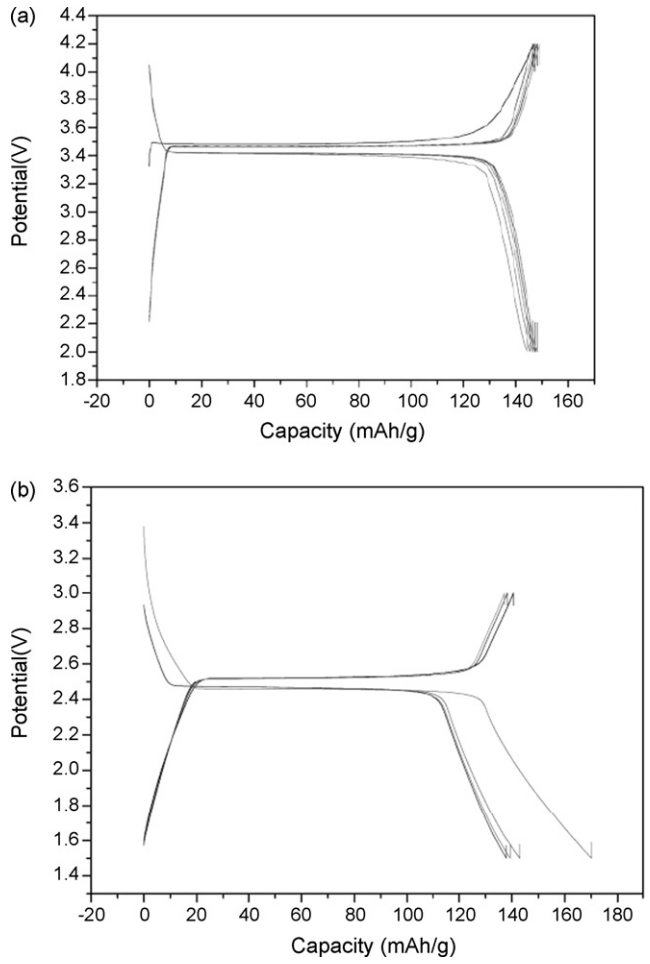

Fig. 4. Charge/discharge profiles of (a) Li//$LiMn_{0.05}Ni_{0.05}Fe_{0.9}PO_4$ and (b) Li//$LiTi_2(PO_4)_3$.

For $LiMn_{0.05}Ni_{0.05}Fe_{0.9}PO_4$//$LiTi_2(PO_4)_3$, organic electrolyte is preferable at low current density. From Fig. 6, it can be seen that the $LiMn_{0.05}Ni_{0.05}Fe_{0.9}PO_4$//$LiTi_2(PO_4)_3$ with organic electrolyte has good cycling performance at a current density of 0.2 mA/cm^2, and a discharge capacity of 103.9 mAh/g was obtained. However, with

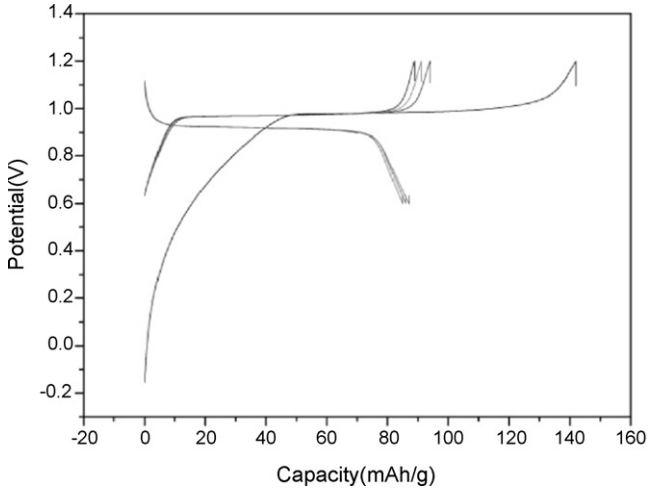

Fig. 5. Charge/discharge profile of $LiMn_{0.05}Ni_{0.05}Fe_{0.9}PO_4$//$LiTi_2(PO_4)_3$ with saturated Li_2SO_4 aqueous electrolyte.

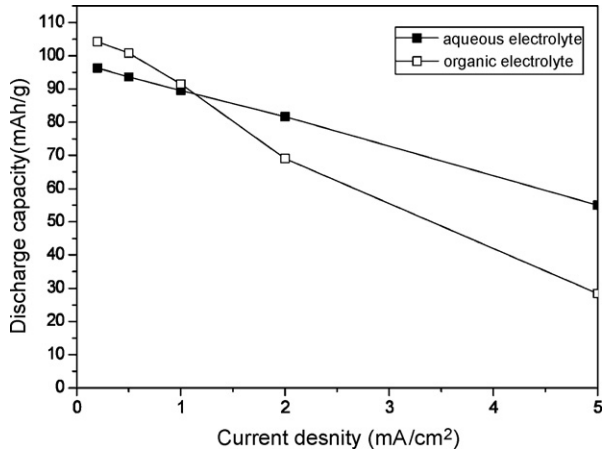

Fig. 6. Rate capabilities of $LiMn_{0.05}Ni_{0.05}Fe_{0.9}PO_4$//$LiTi_2(PO_4)_3$ with different electrolytes.

increases in the current density, the advantage of an aqueous electrolyte could be seen. It appears that the rate capability of aqueous electrolyte is superior to that of organic electrolyte. When the current density was higher than 1.0 mA/cm^2, the rate capability of organic electrolyte decreased severely, while that of aqueous electrolyte decreased relatively slowly. It is a major drawback for any possible applications when cathode and anode materials both have low electronic conductivity, and many efforts have been made to create systems that work efficiently at high current densities. Our results show that aqueous electrolyte provides a promising means of solving this problem.

Fig. 7 shows the cycling performance for $LiMn_{0.05}Ni_{0.05}Fe_{0.9}PO_4$//$LiTi_2(PO_4)_3$ with saturated Li_2SO_4 aqueous solution electrolyte. These data were obtained from constant charge/discharge at a current density of 0.2 mA/cm^2 over the potential range 0.6–1.2 V. The initial discharge capacity obtained at this condition was 87 mAh/g and it is half of the theoretical achievable cathode capacity. The reversible capacity decreased and the discrepancies between the charge and discharge capacity were not small during the first several cycles. However, from them, the discharge/charge efficiency was gradually recovered up to 98%. Li and Dahn have reported that the discharge capacity of a $LiMn_2O_4$//VO_2 battery using 5 M $LiNO_3$ solution as electrolyte fades severely after 20 cycles, which they ascribed to the possibility of the decomposition of water and the dissolution of V ion [11]. Although further analyses are needed to elucidate the cause of the insufficient cyclability, we

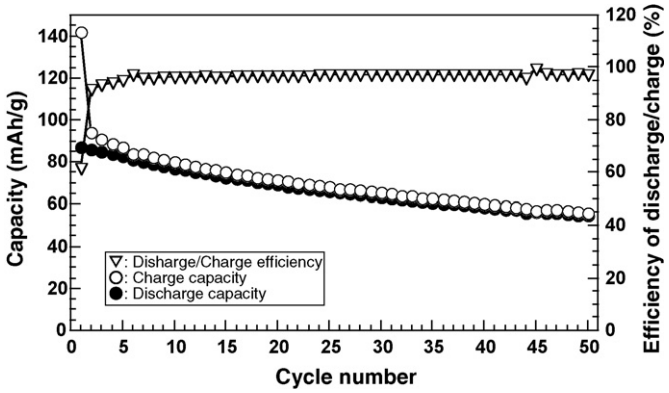

Fig. 7. Discharge/charge capacities and the efficiencies on cycle for the $LiMn_{0.05}Ni_{0.05}Fe_{0.9}PO_4$//$LiTi_2(PO_4)_3$ cell within saturated Li_2SO_4 aqueous solution electrolyte.

have not detected yet any trace of oxygen and hydrogen generation from water and dissolving of metal ions into the electrolyte. In addition, the electrolyte was still colorless and neutral even in the cycled cells.

4. Conclusion

Aqueous cells have been made using $LiMn_{0.05}Ni_{0.05}Fe_{0.9}PO_4$ as cathode material, $LiTi_2(PO_4)_3$ as anode material, and saturated Li_2SO_4 aqueous solution as electrolyte. By controlling the cycle voltage range, no oxygen or hydrogen was generated to destroy the cell. The flat voltage plateaus indicate a two-phase mechanism for lithium insertion/deinsertion. The present results indicate that the rate capability of an aqueous cell is much better than that obtained with organic electrolyte. As such, aqueous lithium ion battery with two-phase cathode/anode electrodes can provide an inexpensive, secure and high rate rechargeable next-generation power sources.

References

[1] T. Lam, R. Louey, J. Power Sources 158 (2006) 1140.
[2] A.W. Stienecker, T. Stuart, C. Ashtiani, J. Power Sources 156 (2006) 755.
[3] C. Deng, P.F. Shi, S. Zhang, Electrochem. Solid State Lett. 9 (2006) A303.
[4] T. Horiba, K. Hironaka, T. Matsumura, J. Power Sources 119 (2006) 893.
[5] K. Smith, C.Y. Wang, J. Power Sources 161 (2006) 628.
[6] K. Smith, C.Y. Wang, J. Power Sources 160 (2006) 662.
[7] I. Belharouak, W.Q. Lu, D. Vissers, K. Amine, Electrochem. Commun. 8 (2006) 329.
[8] K. Zaghib, J. Shim, A. Guerfi, P. Charest, K.A. Striebel, Electrochem. Solid State Lett. 8 (2005) A207.
[9] K. Zaghib, K. Striebel, A. Guerfi, J. Shim, M. Armand, M. Gauthier, Electrochem Acta 50 (2004) 263.
[10] W. Li, J.R. Dahn, D.S. Wainwright, Science 264 (1994) 1115.
[11] W. Li, J.R. Dahn, J. Electrochem. Soc. 142 (1995) 1742.
[12] J. Kohler, H. Makihara, H. Uegaito, H. Inoue, M. Toki, Electrochim. Acta 46 (2000) 59.
[13] Y.G. Wang, Y.Y. Xia, Electrochem. Commun. 7 (2005) 1138.
[14] G.X. Wang, S. Zhong, D.H. Bradhurst, S.X. Dou, H.K. Liu, J. Power. Source 74 (1998) 198.
[15] N.C. Li, C.J. Patrissi, G.L. Che, C.R. Martin, J. Electrochem. Soc. 147 (2000) 2044.
[16] W. Li, W.R. Mckinnon, J.R. Dahn, J. Electrochem. Soc. 141 (1994) 2310.
[17] M. Jayalakshmi, M.M. Rao, F. Scholz, Langmuir 19 (2003) 8430.
[18] M. Manickam, P. Singh, S. Thurgate, K. Prince, J. Power Source 158 (2006) 646.
[19] M. Manickam, P. Singh, S. Thurgate, K. Prince, Electrochem. Solid-State Lett. 9 (2006) A471.
[20] S. Okada, J. Yamaki, J. Ind. Eng. Chem. 10 (2004) 1104.
[21] X.H. Liu, J.Q. Wang, J.Y. Zhang, S.R. Yang, Chin. J. Chem. Phys. 19 (2006) 530.
[22] S. Patoux, C. Masquelier, Chem. Mater. 14 (2002) 5057.